ACCOUNTS of chemical research

Article

pubs.acs.org/accounts

Spherical Colloidal Photonic Crystals

Yuanjin Zhao,* Luoran Shang, Yao Cheng, and Zhongze Gu*

State Key Laboratory of Bioelectronics, School of Biological Science and Medical Engineering, Southeast University, Nanjing 210096, China

CONSPECTUS: Colloidal photonic crystals (PhCs), periodically arranged monodisperse nanoparticles, have emerged as one of the most promising materials for light manipulation because of their photonic band gaps (PBGs), which affect photons in a manner similar to the effect of semiconductor energy band gaps on electrons. The PBGs arise due to the periodic modulation of the refractive index between the building nanoparticles and the surrounding medium in space with subwavelength period. This leads to light with certain wavelengths or frequencies located in the PBG being prohibited from propagating. Because of this special property, the fabrication and application of colloidal PhCs have attracted increasing interest from researchers. The most simple and economical method for fabrication of colloidal PhCs is the bottom-up approach of nanoparticle self-assembly. Common colloidal PhCs from this approach in nature are gem opals, which are made from the ordered assembly and deposition of spherical silica nanoparticles after years of siliceous sedimentation and compression. Besides naturally occurring opals, a variety of manmade colloidal PhCs with thin film or bulk morphology have also been developed. In principle, because of the effect of Bragg diffraction, these PhC materials show different structural colors when observed from different angles, resulting in brilliant colors and important applications. However, this angle dependence is disadvantageous for the construction of some optical materials and devices in which wide viewing angles are desired.

Recently, a series of colloidal PhC materials with spherical macroscopic morphology have been created. Because of their spherical symmetry, the PBGs of spherical colloidal PhCs are independent of rotation under illumination of the surface at a fixed incident angle of the light, broadening the perspective of their applications. Based on droplet templates containing colloidal nanoparticles, these spherical colloidal PhCs can be generated by evaporation-induced nanoparticle crystallization or polymerization of ordered nanoparticle crystallization arrays. In particular, because microfluidics was used for the generation of the droplet templates, the development of spherical colloidal PhCs has progressed significantly. These new strategies not only ensure monodispersity, but also increase the structural and functional diversity of the PhC beads, paving the way for the development of advanced optoelectronic devices.

In this Account, we present the research progress on spherical colloidal PhCs, including their design, preparation, and potential applications. We outline various types of spherical colloidal PhCs, such as close-packed, non-close-packed, inverse opal, biphasic or multiphasic Janus structured, and core−shell structured geometries. Based on their unique optical properties, applications of the spherical colloidal PhCs for displays, sensors, barcodes, and cell culture microcarriers are presented. Future developments of the spherical colloidal PhC materials are also envisioned.

1. INTRODUCTION

Photonic crystals (PhCs) are structured materials that have spatial periodicity in their dielectric constant. These materials can strongly modulate electromagnetic waves and with sufficient dielectric contrast and appropriate geometry may exhibit a photonic band gap (PBG). Similar to the electronic band gap in semiconductors, PhC materials offer the possibility of manipulating photons with the energy in their PBG. Therefore, PhCs potentially offer revolutionary advances in next-generation microphotonic devices.[1,2] Over the past two decades, there has been much interest in exploring new PhC materials and studying their related new phenomena. The existing techniques for the fabrication of PhCs can be roughly classified into top-down and bottom-up approaches. The top-down approach involves using macroscopic tools to first transfer a computer-generated pattern onto a larger piece of bulk material, and then "sculpting" a nanostructure by physically removing material, or using macroscopic tools to directly "write" materials on a substrate. Based on these strategies, a wide range of high-quality photonic nanostructures with arbitrary complexity was achieved. However, the high cost, low time efficiency, and some technological limitations still restrict the mass production of PhC materials using these approaches. In contrast, the bottom-up approaches take advantage of physicochemical interactions for the hierarchical synthesis of ordered nanostructures through the self-assembly of basic building blocks. They are low cost, time effective, and not restricted by the nanoscales.

Received: August 26, 2014
Published: November 13, 2014

   dx.doi.org/10.1021/ar500317s | *Acc. Chem. Res.* 2014, 47, 3632−3642

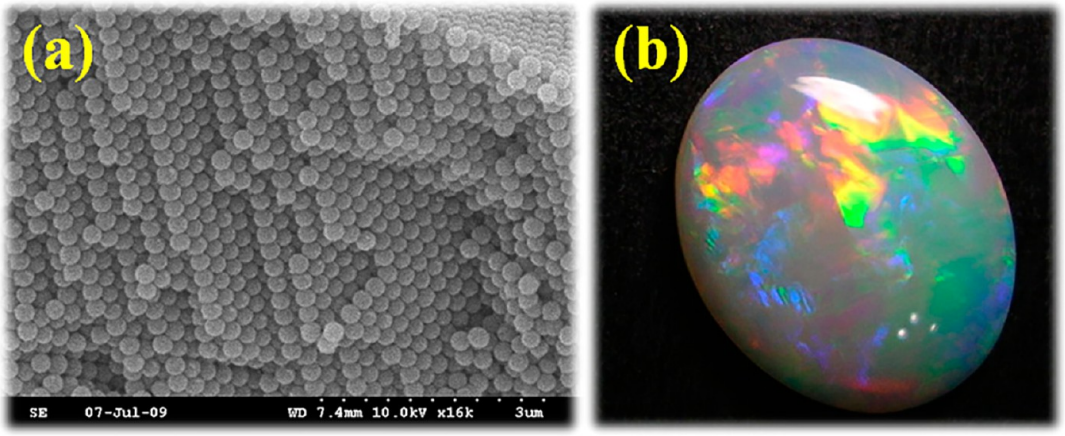

Figure 1. (a) Typical SEM image of colloidal crystals; (b) a natural opal.

Table 1. General Comparison between Different PCBs from Various Aspects

topology	PhC nanostructure	synthetic template	solidification method	ref
uniform PCBs	close-packed CCA	single emulsion	solvent evaporation	7, 9−15, 38, 46
	non-close-packed CCA	single emulsion	photopolymerization	16−19
	inverse opal	close-packed PCBs	etching	20−27, 44, 47
Janus or multicomponents	close-packed CCA	Janus emulsion	solvent evaporation	28−31
	non-close-packed CCA	multicomponent emulsion	photopolymerization	19, 32, 40
core−shell structures	non-close-packed CCA	double emulsion	photopolymerization	33−36, 41, 45
	close-packed CCA and their inverse structure	close-packed PCBs	controlled etching	37, 52

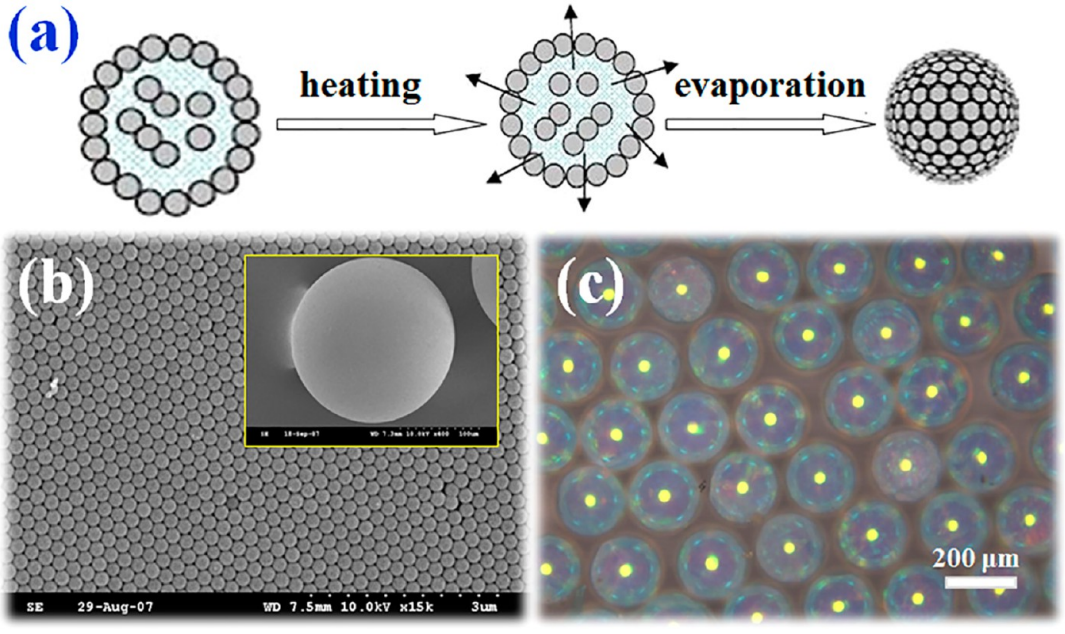

Figure 2. (a) Schematic illustration of the close-packed colloidal PCBs generation. (b) SEM image of the bead surface; the inset is an image of a bead. (c) Reflection image of the PCBs.

Among different kinds of bottom-up approaches, the assembly or crystallization of monodisperse colloidal nanoparticles into organized arrays, so-called colloidal crystals (Figure 1a), is the most promising technique for preparing PhC materials.[3−6] A prototype of the colloidal PhC materials in nature is gem opals (Figure 1b), which are made from the ordered deposition of spherical silica nanoparticles after years of siliceous sedimentation and compression under hydrostatic and gravitational forces. Gem opals usually have irregular macroscopic appearance. Unlike naturally occurring opals, most manmade colloidal PhCs are made into thin film or bulk materials to meet the requirements of different applications. In these materials, the nanoparticles mainly form a face-centered cubic (FCC) structure, which is the thermodynamically stable position with minimum free energy. The PBGs of the colloidal PhCs could be estimated from the Bragg−Snell equation:

$$\lambda = 2D(n_{\text{eff}}{}^2 - \cos^2\theta)^{1/2} \quad (1)$$

dx.doi.org/10.1021/ar500317s | Acc. Chem. Res. 2014, 47, 3632−3642

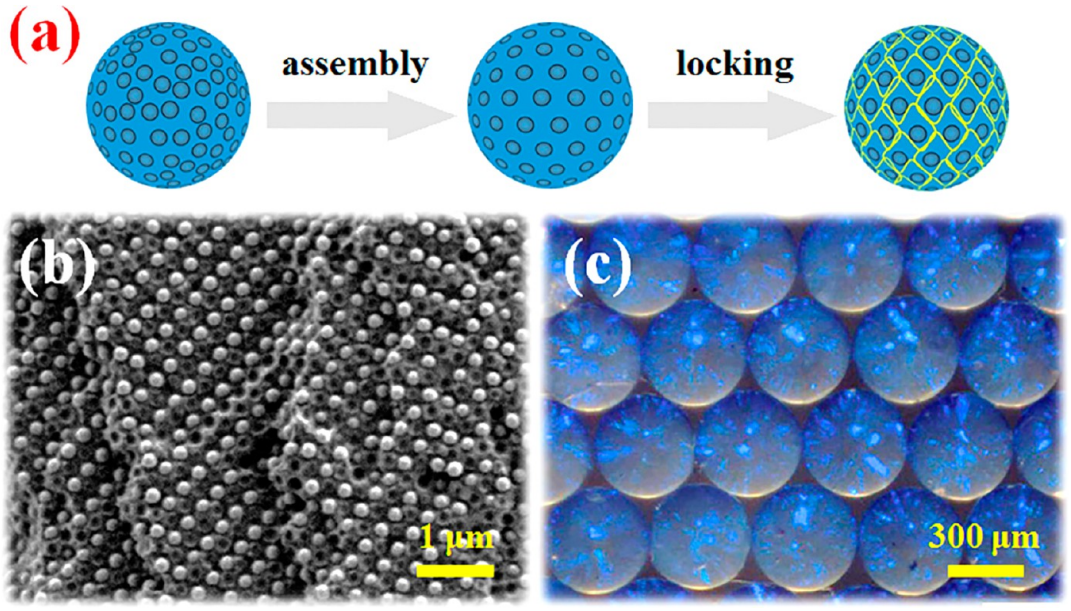

Figure 3. (a) Schematic of the non-close-packed colloidal PCBs generation. (b,c) SEM image and photograph of the non-close-packed PCBs. Panel (c) reproduced from ref 16 with permission of The Royal Society of Chemistry.

where λ is the wavelength of the reflected light, n_{eff} is the average refractive index of the constituent colloidal crystals, D is the distance of diffracting plane spacing, and θ is the Bragg angle of incidence of the light falling on the PhC nanostructures. From eq 1, it could be found that colloidal PhC films show different reflection wavelengths and structural colors when observed from different angles. This feature imparts PhC materials with brilliant colors for many applications.[6] However, this angle dependence is disadvantageous for the construction of some optical materials and sensor devices in which wide viewing angles are desired.

Recently, a series of new colloidal PhC materials with spherical macroscopic appearance have been developed.[7,8] Because of the spherical symmetry, their PBGs and reflection wavelengths are independent of the rotation under illumination of the surface at a fixed incident angle of the light, broadening their range of applications. Based on droplet templates containing colloidal nanoparticles, these spherical colloidal PhCs could be generated by simple methods such as evaporation-induced nanoparticle crystallization or polymerization of ordered nanoparticle crystallization arrays. In particular, because microfluidics was used for the generation of the droplet templates, the development of spherical colloidal PhCs has significantly progressed. These new strategies not only ensure monodispersity, but also increase the structural and functional diversity of the PhC beads (PCBs), paving the way for the development of advanced optoelectronic devices.

In this Account, we present the research progress on spherical colloidal PhCs. After introducing the general fabrication strategies of the different colloidal PCBs, we focus on studies of the features and applications of these materials. Examples of typical PCBs are presented and typical applications of these PhC materials in different areas are described. Finally, the outlook for the future development of PCBs is presented.

2. TAILORING SPHERICAL COLLOIDAL PhCs

Based on the topology of the spherical colloidal PhCs, PCBs could be classified into three categories, including PCBs with uniform structures, PCBs with Janus or multicomponent structures, and PCBs with core−shell structures (Table 1). The PhC nanostructures of these PCBs include close-packed colloidal crystal array (CCA), non-close-packed CCA or inverse opal.

2.1. Colloidal PCBs with Uniform Structures

Close-Packed Colloidal PCBs. Close-packed colloidal PCBs are essentially spherical colloidal crystal clusters. Evaporation-induced crystallization of colloidal nanoparticles is the most popular approach to form PCBs from droplet templates (Figure 2).[9,10] Intrinsically, evaporation-induced colloidal assembly can be regarded as a concentration process, in which the volume fraction of building blocks gradually increases from a low value to a maximum (74%). In this process, capillary forces provide a compressive force that is spherically symmetrical and ultimately leads to the arrangement of the colloidal nanoparticles. The capillary forces thus close-pack the nanoparticles into their final spherical configuration, and the van der Waals forces subsequently cement the nanoparticles together. Similar to the colloidal crystals in a plane, the surfaces of the PCBs also form the (111) plane of the FCC symmetry. Because of the surface curvature, the PhC bead has intrinsic defects and grain boundaries. However, when the diameter of the bead is much larger than the colloidal size (more than hundreds of times), the curvature effects on the crystallization become negligible.

The size of the PCBs is determined by the initial droplet template size and the nanoparticle volume fraction in the initial droplet. Thus, to fabricate uniform beads, monodisperse droplets are required, which can be prepared using a microfluidic device. Based on the microfluidic droplets, uniform PCBs could be fabricated with different organic and inorganic nanoparticles as their basic building blocks by slowly evaporating the solvent of the droplets.[11,12] To reduce the evaporation time, microwave irradiation was used for heating, which can selectively superheat polar molecules and consolidate the PCBs within a very short time.[13] In addition, the fast

dx.doi.org/10.1021/ar500317s | Acc. Chem. Res. 2014, 47, 3632−3642

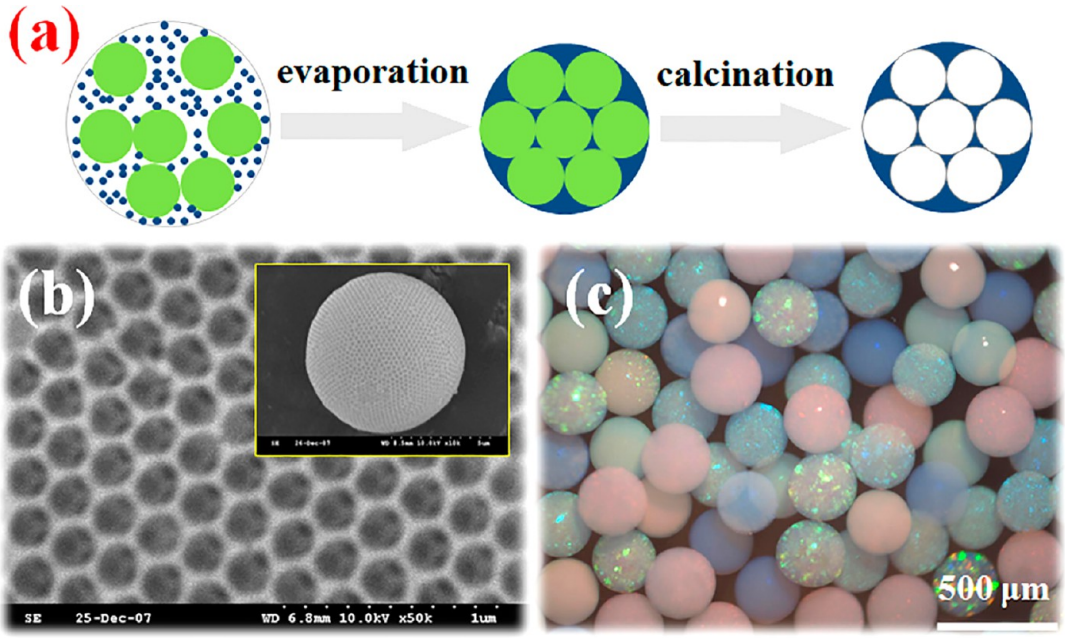

Figure 4. (a) Schematic of the generation of the spherical inverse opal. (b) SEM image of the inverse opal bead surface; the inset is the image of a bead. (c) Photograph of the mixture of seven kinds of inverse opal beads. Panel (c) reproduced from ref 26. Copyright 2009 WILEY-VCH Verlag GmbH & Co. KGaA, Weinheim.

solidification of the PCBs could also be realized by using a solvent-extraction method.[14]

It is worth noting that despite being solidified and close-packed, the PCBs were fragile when the assembled nanoparticles were attached via the van der Waals force, which was too weak to hold the nanoparticles together under mixing or vibration. To solve this problem, the PCBs were treated by thermal sintering. At temperatures somewhat above the glass transition temperature, polymeric or silica colloids become viscoelastic and slightly fuse with neighboring nanoparticles to form a neck structure. With this treatment, the mechanical strength of the PCBs increased dramatically and the resultant beads may be stable for shaking, mixing, and even sonication experiments.[15]

Non-Close-Packed Colloidal PCBs. PCBs with non-close-packed colloidal crystal nanostructure could be fabricated by water or oil droplet templates that containing colloidal nanoparticles.[16−18] When some charged colloidal nanoparticles are encapsulated in a pure water droplet in relatively high concentration, significant interparticle repulsion occurs at the average interparticle spacing, and the minimum energy configuration makes the colloidal nanoparticles self-assemble into a non-close-packed FCC or body-centered cubic (BCC) CCA structure in the droplet templates. Because of the periodic arrangement of the nanoparticles, the droplet templates were imparted with the PBG property. Although the CCA can be stable for a long time, it will transiently become disordered under shock or upon introduction of ionic impurities. This restricts the application of the CCA droplets. As an innovation, highly purified nonionic polymerizable monomers, such as poly(ethylene glycol) diacrylates (PEG-DA) and *N*-isopropylacrylamide (NIPAm), which can form a hydrogel network around the CCA nanoparticles, were used for the droplet templates. With this method, the CCA was permanently locked in a hydrogel matrix (Figure 3).[16] Because the CCA no longer depends on electrostatic interactions between the nanoparticles, the resultant non-close-packed colloidal PCBs remain stable in a different, disturbed surrounding medium.

The non-close-packed CCA could also form in nonpolar oil phases. This was realized by using the evaporation of a volatile solvent, in which the nanoparticles could be easily dispersed, in a target oil phase with a higher boiling point. With a high concentration in the target oil phase, the nanoparticles self-assemble into a CCA structure because of the balance between long-range attraction and electrostatic repulsion of the neighboring charged nanoparticles. When used for the fabrication of PCBs, ethoxylated trimethylolpropane triacrylate (ETPTA), a photocurable resin, was the oil used for the dispersing and self-assembling of the silica nanoparticles. This resin solution could be emulsified and subsequently solidified in the droplet microfluidic device equipped with an ultraviolet (UV) exposure unit. The solidified silica-in-ETPTA PCBs contained the same ordered non-close-packed CCA structure as their emulsion templates, and thus showed bright structural colors.[19]

Spherical Inverse Opals. Similar to the inverse opal film, inverse opal beads could be fabricated by template replication or coassembly. In the process of replicating, the materials of which the final inverse opal specimen should consist are filled into the free voids of the templates. These filled materials for inverse opal film fabrication included ultrafine nanoparticles (that are much smaller than the channels of the free voids), precursors of metal oxide, prepolymer solution of hydrogels, and so forth.[20−23] However, during the fabrication of the inverse opal beads by rigid materials, the colloidal crystal bead templates should be fully embedded in the rigid materials to achieve a complete filling, making it impossible to release the hybrid or inverse opal beads from the materials.[20] In contrast, soft hydrogel materials could be torn without destroying the colloidal crystal bead templates, thus the hybrid beads could be separated from the hydrogel even they were complete embed. After etching the nanoparticles, inverse opal hydrogel beads with a perfect spherical geometry could be achieved.

dx.doi.org/10.1021/ar500317s | *Acc. Chem. Res.* 2014, 47, 3632−3642

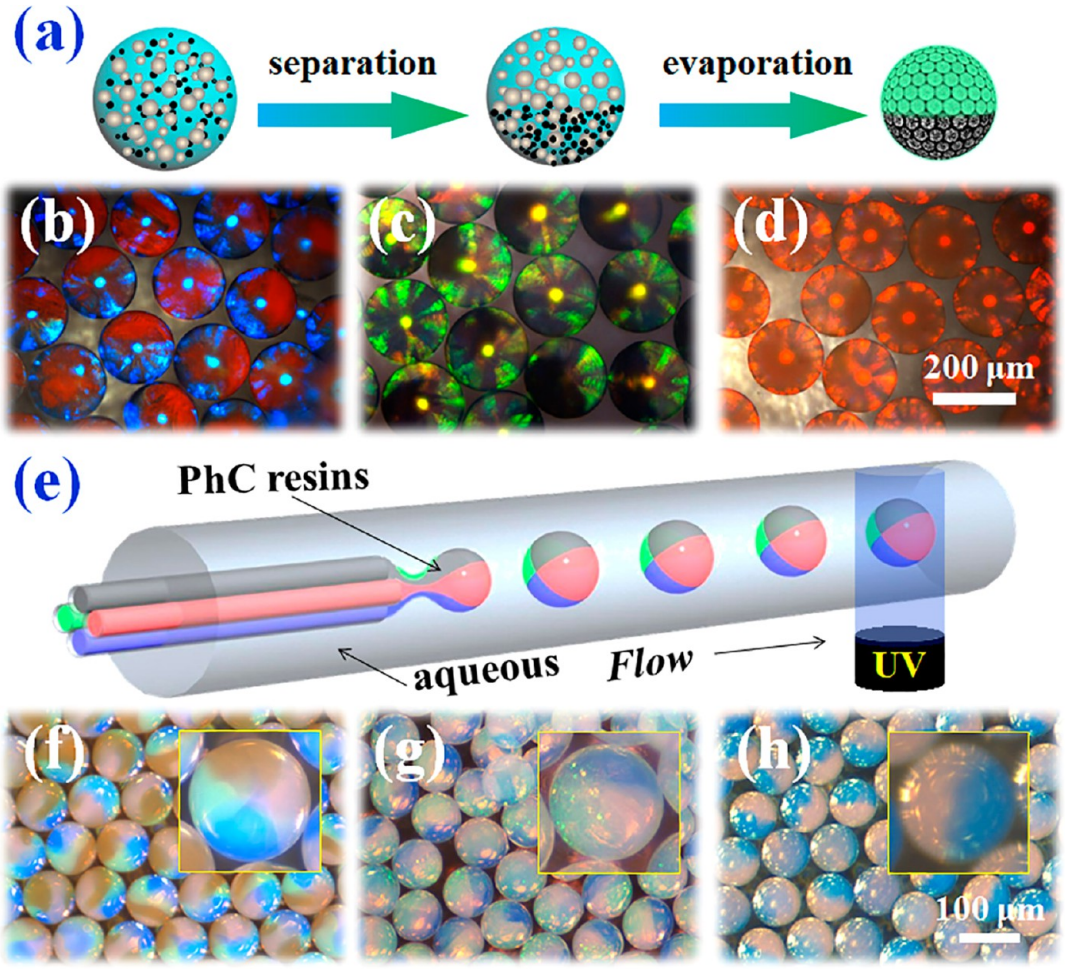

Figure 5. (a–d) Janus PCBs from phase separation of nanoparticles in droplets. Reproduced from ref 30 with permission of The Royal Society of Chemistry. (e–h) Janus PCBs from the polymerization of multiphasic single-droplet templates. Reprinted with permission from ref 32. Copyright 2013 American Chemical Society.

Another approach for spherical inverse opal fabrication is coassembly (Figure 4a), which represents concurrent processes of formation of colloidal crystal bead template and simultaneous filling of the interstitial sites with the desired framework materials.[24−27] It is usually achieved by the evaporation of droplets that contain a mixture of the templating polystyrene nanoparticles with a matrix of ultrafine silica nanoparticles. Theoretically, when the polystyrene nanoparticles that are packed closely to a bead in an FCC arrangement and the ultrafine silica nanoparticles infiltrate all the interstitial sites between the polystyrene nanoparticles, the volume ratio of polystyrene and silica nanoparticles should be about 3.85. However, during evaporation, the polystyrene nanoparticles escape more easily than the silica nanoparticles from the droplet templates, and after solidification, the silica nanoparticles cannot infiltrate all the interstitial sites between the polystyrene nanoparticles, and the practical volume ratio for achieving an ideal coassembly is about 9. By removing the polystyrene templates, spherical silica inverse opals could also be generated (Figure 4b, c).[26]

2.2. PCBs with Janus or Multicomponent Structures

Microparticles having a biphasic geometry of distinct compositions and properties are known as "Janus" beads. PCBs with these structures can have diverse functions because of their anisotropic nature. Janus PCBs could be prepared by phase separation of colloidal nanoparticles within droplet templates.[28−30] For instance, aqueous droplets containing monodisperse silica nanoparticles and ultrafine magnetic nanoparticles exhibit phase separation under a magnetic field. When these droplets are dried in an oven, the silica nanoparticles in the templates self-assemble into close-packed spherical CCA structure to achieve the lowest energy state, and the ultrafine magnetic nanoparticles infiltrate the interstitial sites between the silica nanoparticles in the bottom hemispheres, as schemed in Figure 5a. Janus PCBs with the features of an anisotropic PBG structure and magnetic properties were achieved after these processes (Figure 5b–d).[30]

Janus PCBs could also be achieved by biphasic or multiphasic single-droplet templates that consist of two or more separate domains.[19,31] These emulsion templates were prepared by using capillary microfluidic devices in which distinct fluids were injected using multibarreled capillaries in parallel with an angular distribution. The fluids could be silica-in-ETPTA solutions with different structural colors. These miscible fluids formed several parallel flows in the microfluidic channel and were emulsified into multiphasic droplet templates at a junction at which a continuous phase exerted a drag force on the parallel streams. The generated droplet templates maintained their compartments for some distance as they flowed through symmetric channels. After polymerization, solidified PCBs with

dx.doi.org/10.1021/ar500317s | Acc. Chem. Res. 2014, 47, 3632−3642

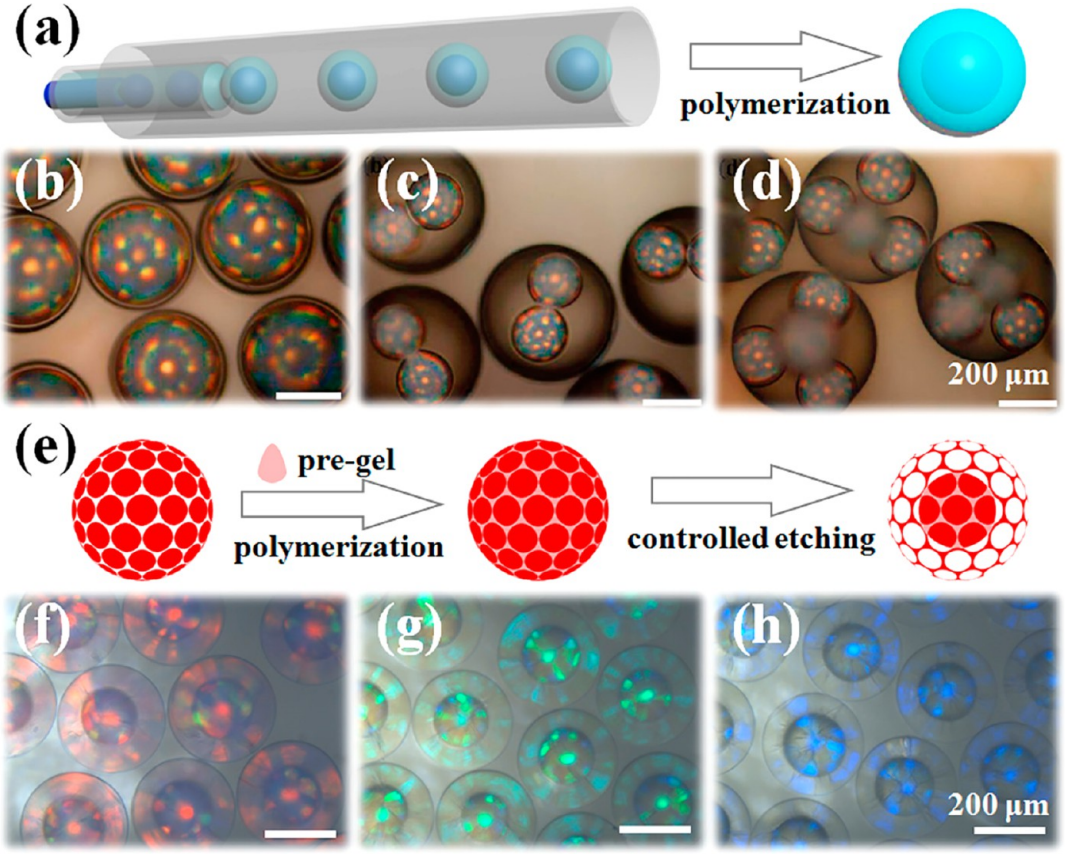

Figure 6. (a–d) Double emulsion templated PhC capsules with non-close-packed CCA cores and ETPTA shells. Reprinted with permission from ref 33. Copyright 2008 American Chemical Society. (e–h) Etching resultant core–shell structured PCBs with opal cores and inverse opal hydrogel shells. Reproduced from ref 37. Copyright 2014 WILEY-VCH Verlag GmbH & Co. KGaA, Weinheim.

the corresponding multiphasic geometry were generated (Figure 5e–h).[32] To achieve additional functionality of the Janus PCBs, magnetic or carbon-black nanoparticles could also be dispersed in one part of the multiphasic emulsion droplets for the generation of beads controllable by the external field.

2.3. Core–Shell Structured PCBs

Besides single emulsion droplets, double emulsion droplets, in which dispersed droplets contain smaller droplets inside, could also be used as templates for the generation of PCBs.[33−36] Based on these templates core–shell structured PCBs could be achieved. For example, with a stepwise emulsification droplet microfluidic device, the aqueous solutions containing non-close-packed CCAs could be encapsulated using an ETPTA resin (Figure 6a–d).[33] In this situation, the ETPTA formed a rigid shell to preserve the core droplets; thus, the core of the PCBs could disperse bright structure colors even without locking their CCAs by a hydrogel matrix. Based on the same method, the PCBs with a non-close-packed CCA in their shell layer could also be generated by using the nanoparticle-dispersed solutions as the middle encapsulating phase.[36] In this case, the CCA should be well locked to improve the stability of the PhC structure as the above non-close-packed colloidal PCBs.

The core–shell structured PCBs could also be generated by replicating and etching the silica colloidal crystal bead templates like the approach of spherical inverse opal fabrication. As the etching process of the template silica nanoparticles was gradual, from the outer to the inner sphere, the core–shell structured PCBs could be achieved when the etching times of the hybrid beads were well controlled (Figure 6e–h).[37] The resultant PCBs were composed of close-packed opal PhC cores and inverse opal PhC hydrogel shells. The different relative refractive indexes of the shell and core created two distinct PBGs in these core–shell structured PCBs.

3. APPLICATIONS

3.1. Displays

Because of their unique optical characteristics, the PCBs can be used as basic units to fabricate display materials or devices. Unlike most of the existing emissive displays, which are poorly visible in bright sunlight, the PhC-based technologies are reflective displays and thus can overcome this restriction. To realize this concept, PCBs were assembled into films or used as separated units.[38,39] The spherical PhC-composed films had structural colors similar to their spherical PhC elements and showed constant colors at different viewing angles. This was different from the colloidal PhC film, which showed an obvious color variation at different viewing angles. Attractively, by using the PEG hydrogel to replicate the spherical PhC-composed films, a novel photonic paper with features of flexible texture, vivid colors, wide viewing angles, and rewritable surfaces could be achieved for potential information displays (Figure 7a, b).[38]

When used as separated display units, the PCBs were placed in a highly ordered hole array on a substrate and the color of every PhC bead unit could be turned by external fields.[31,32,40] For instance, by using the Janus PCBs that consisted of a structural color hemisphere and magnetic nanoparticles, or a carbon-black containing hemisphere as the display units, the

dx.doi.org/10.1021/ar500317s | Acc. Chem. Res. 2014, 47, 3632−3642

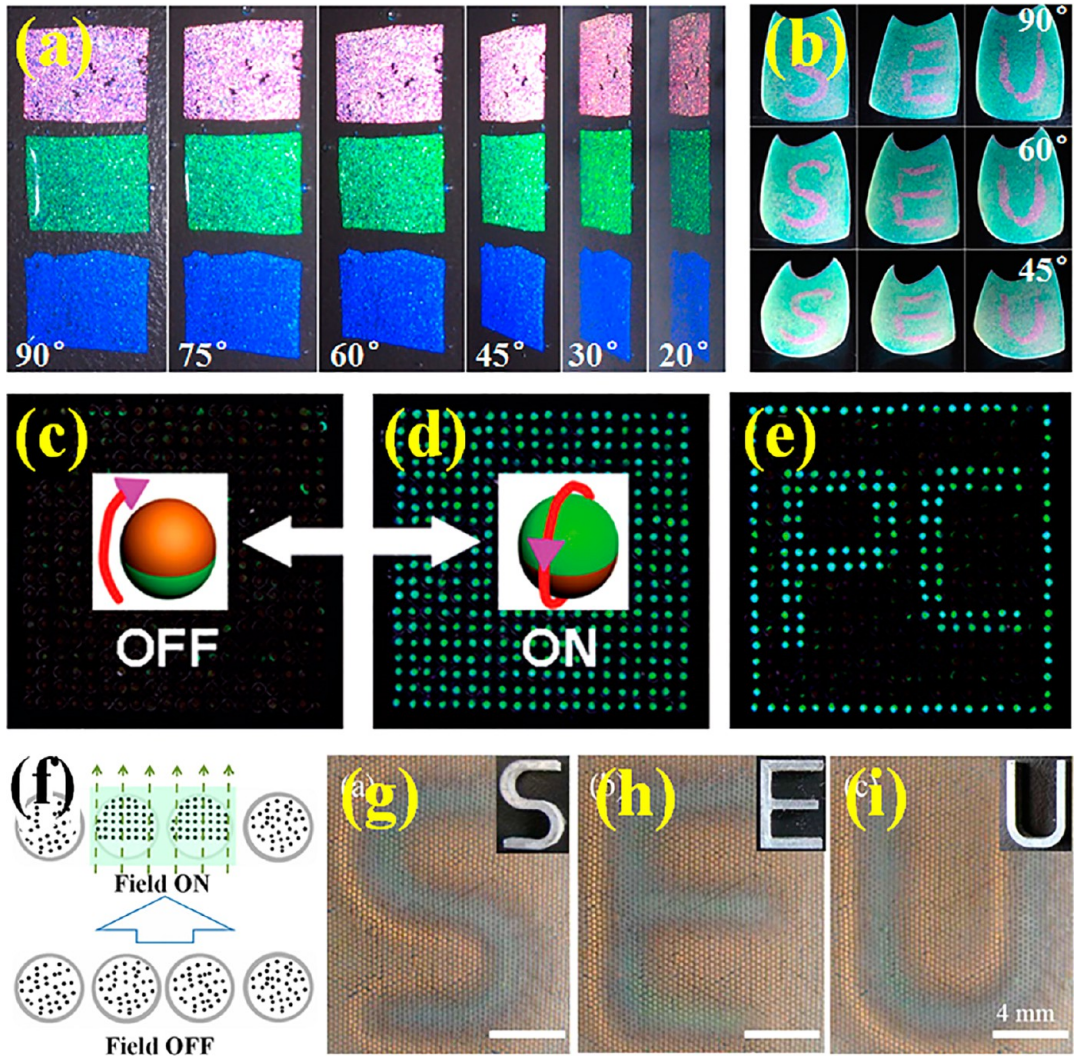

Figure 7. (a,b) Photonic papers (replicated from spherical PhC-composed films) and their ink marks show angle-independence. Reproduced from ref 38. Copyright 2013 WILEY-VCH Verlag GmbH & Co. KGaA, Weinheim. (c–e) magnetic Janus PCBs for the "gray" and "color" display. Reproduced from ref 31. Copyright 2012 WILEY-VCH Verlag GmbH & Co. KGaA, Weinheim. (f–i) PhC microcapsules with rigid ETPTA shells and magnetic nanoparticles-contained cores for dynamically full color displays. Reproduced from ref 41. Copyright 2011 WILEY-VCH Verlag GmbH & Co. KGaA, Weinheim.

substrate could display "gray/dark" and "color" with control of the direction of the magnetic or electric fields (Figure 7c–e). Patterns such as letters or characters could also be displayed in the substrate by using a magnetic pen or patterned external fields.[31] To realize the dynamically full color displays, PhC microcapsules with rigid ETPTA shells and magnetic or highly charged nanoparticles containing cores should be used as the display units. The nanoparticles in the core droplet could be influenced by an external magnetic field, forming ordered CCA structures with different diffracting spacing, and therefore various distinct colors could be displayed according to the intensity of the external fields (Figure 7f–i).[41]

3.2. PhC Barcodes

The increasing use of high-throughput assays in biomedical applications demands effective strategies for multiplexing. One promising strategy is to use barcode particles that encode information about their specific compositions and enable simple identification (Figure 8a). Among the various barcode particles, spectroscopic barcodes, such as fluorescent dyes and quantum dots, are the most established because of their simplicity in both encoding and detection. However, these particles present some disadvantages, including photobleaching during storage and the potential interference of encoding fluorescence with analyte-detection fluorescence. Recently, PCBs have been applied as a new type of spectroscopic barcode, with codes that are the characteristic reflection peaks originating from the PBGs. As the peak positions are based on their periodical physical structure, the codes are very stable and the fluorescence background is relatively low.[42]

Generally, PhC barcodes with dozens of distinctive encoded reflection peaks could be obtained by using different sizes of silica nanoparticles for their assemblage (Figure 8b).[15] As the surface was arranged by hexagonal symmetry nanoparticles, the PhC barcodes could provide not only more surface area for probe immobilization and reaction, but also a nanopatterned platform for highly efficient bioreactions.[43] The sensitivity of the PhC barcodes could be further improved by using a bioinert hydrogel for the composed materials of the particles, which provided homogeneous water surroundings for bioreactions.[44] An effective strategy for increasing the identification codes of

dx.doi.org/10.1021/ar500317s | Acc. Chem. Res. 2014, 47, 3632–3642

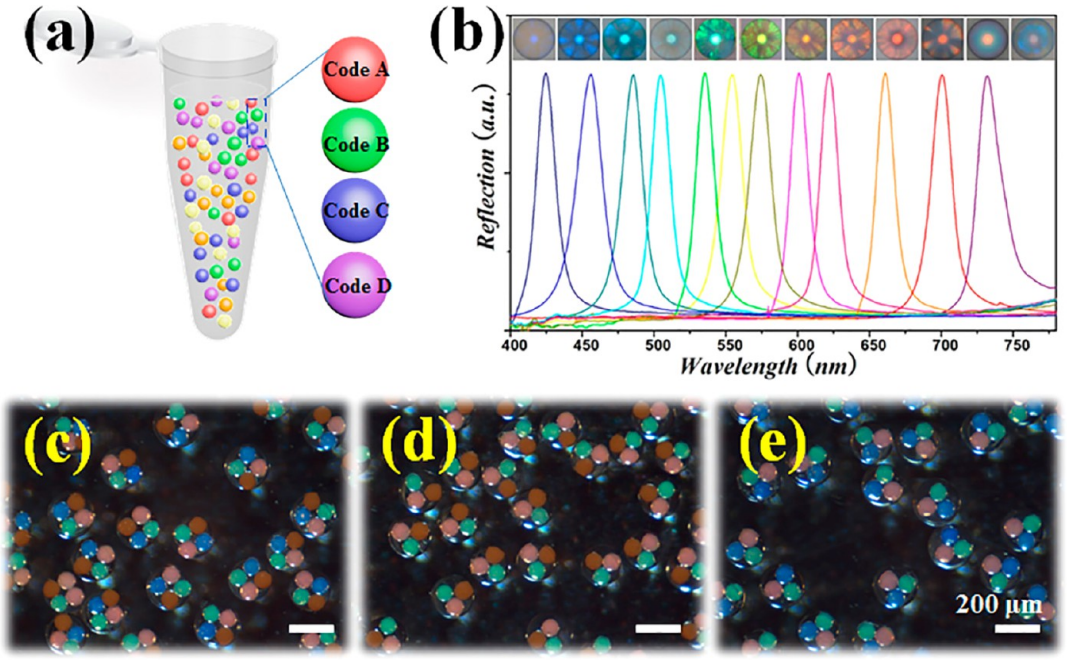

Figure 8. (a) Schematic of barcode particle-based multiplexing. (b) Optical micrographs and reflection spectra of 12 kinds of PhC barcodes. (c–e) Photographs of the PhC barcodes with multiple PhC-tagged resin cores. Reprinted by permission from Macmillan Publishers Ltd: *NPG Asia Materials* (ref 45), copyright 2012.

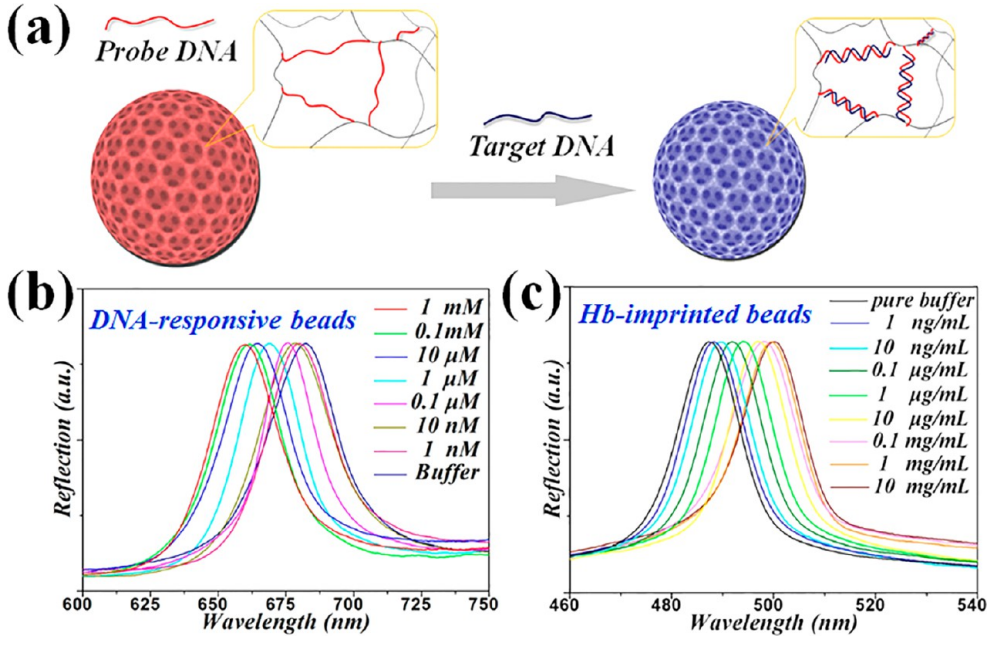

Figure 9. (a) Schematic of the hydrogel inverse opal beads for label-free sensing. (b,c) Optical responses of responsive PCBs to different concentrations of target DNA and protein, respectively.

the particles was to encapsulate multiple PhC-tagged resin cores into hydrogel shells (Figure 8c–e).[45] As each core has distinct reflection peaks, the composed PhC barcodes allow for a substantial number of coding levels. Moreover, the presence of magnetism in the barcodes could confer their controllable movement under magnetic fields, which could significantly increase the sensitivity of the bioassays and simplify the processing. These features make PhC barcodes ideal for multiplexing applications.

3.3. Label-Free Sensors

In label-free sensors, target molecules are not labeled and are detected in their natural forms. These types of sensors are not only able to eliminate the time-consuming and expensive labeling steps, but also allow for kinetic measurement of molecular interactions. To carry out label-free assays by PCBs, the interactions of analyte and probes on the beads should result in some physicochemical changes of the beads, such as the average refractive index or diffracting plane spac-

dx.doi.org/10.1021/ar500317s | *Acc. Chem. Res.* 2014, 47, 3632–3642

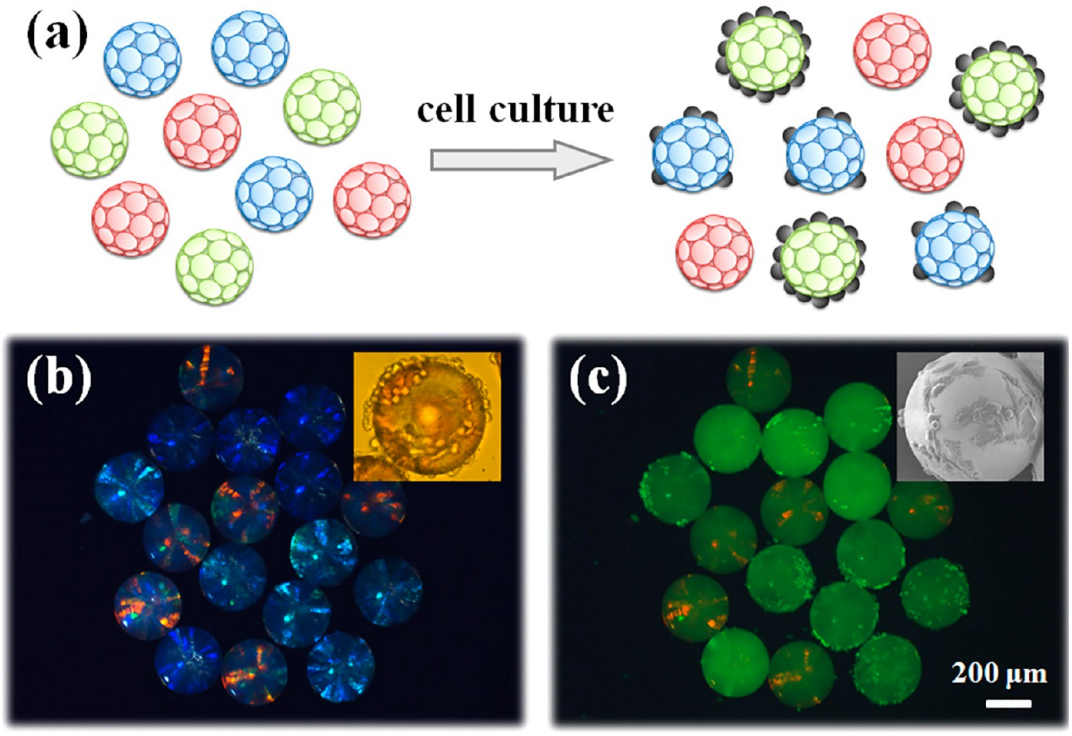

Figure 10. (a) Schematic of the PCBs composed of different biomaterials for multiplexing cells research. (b,c) optical and the corresponding fluorescence images of the PCBs after HepG2 cell culture. Insets are the transmission image and SEM image of the cells on the beads. Reproduced from ref 51. Copyright 2013 WILEY-VCH Verlag GmbH & Co. KGaA, Weinheim.

ing.[20,26,46−50] These changes in the PCBs could be detected as shifts in their PBGs or structural colors.

In the situation of changing the average refraction index, the silica inverse opal beads, which were with interconnected pores for molecular diffusion into their inner structure, were employed. When used in immunoassays, specific binding of tumor markers to their corresponding anticancer probes on the pore surfaces results in increasing the average refractive index of the porous beads and this effect can be detected as a corresponding red shift in the diffraction peak position.[26] The shift value of the peak position can be used to quantitatively estimate the amount of the bound tumor markers.

To improve the detection sensitivity, hydrogel PC beads with an increased response level were used. In this case, the response mechanisms were mainly based on the change in the diffracting plane spacing induced by the external stimuli. For instance, by using DNA-responsive hydrogel or protein-imprinted polymers as the skeleton materials, the resultant inverse opal beads could be used for label-free detection of the matched DNA or proteins (Figure 9).[20,47] A powerful feature of this sensor is that the multiplex label-free assay could be achieved by using a series of PBG-encoded inverse opal beads with different responsive receptors. In this multiplexing, both the decoding and molecule detection were as simple as one-step measurements of the diffraction peak of the inverse opal beads, which simplifies the detection instruments and procedures.

3.4. Cell Microcarriers

PCBs can be used as microcarriers for capture and culture cells.[51,52] The cell microcarrier platform combines the advantages of both adherent and suspension cultures, and is suitable for large-scale cultivation of different cells. Because of these features, many kinds of cell microcarriers have been fabricated using different biomaterials. However, these microcarriers usually perform a single function and cannot be mixed for multiple cell research because they are indistinguishable. Moreover, a series of soft hydrogels, which have poor plasticity, were difficult to be cast into microcarriers for cell culture. To solve these problems, PCBs were used that could not only provide interconnected macropore scaffolds for infiltrating and casting the soft hydrogels, but could also provide distinguishable PhC-encoded information for multiplexing. For example, three kinds of colloidal PCBs with red, green, and blue structural colors were infiltrated with PEG hydrogel, collagen, and blank, respectively. These beads were mixed for the culture of HepG2 cells. Because of the demonstrated promotion- and antiadhesion effects of the collagen and PEG, respectively, the expected observation was that of a large population of HepG2 cells on the green beads, and only a few on the red beads (Figure 10).[51] By decorating their surfaces with highly branched dendrimer-amplified aptamer probes, the colloidal PCBs could also be employed for capturing and detecting multiple circulating tumor cells (CTCs).[52] These results indicate the advantages of PCBs in cell research.

4. SUMMARY AND OUTLOOK

This Account summarizes some recent advances that focus on the fabrication of spherical colloidal PhCs and their applications. The colloidal PCBs with a series of micro- and nanostructures, including close-packed, non-close-packed, inverse opal, biphasic or multiphasic Janus geometries, and core−shell geometries, have been generated by solvent evaporation-induced crystallization, in situ photopolymerization, or template replication. It is of great importance that a combination of various techniques such as microfluidics, optofluidics, as well as intelligently responsive materials was created to endow the monodisperse PCBs with novel functions.

dx.doi.org/10.1021/ar500317s | Acc. Chem. Res. 2014, 47, 3632−3642

Based on these functions, various applications of the PCBs in displays, sensors, barcodes, and cell culture microcarriers have been achieved, opening a new chapter for PhC materials.

The research on spherical PhCs is still ongoing, and numerous challenges remain in their development. First, although the PCBs could be fabricated continuously by microfluidics, bulk generation of the monodisperse beads is out of reach for practical applications, and thus advanced emulsification technology, such as improved membrane emulsification and parallel microfluidics, is anticipated to mass-produce the droplet templates and their derived beads. Second, it is necessary to design, synthesize, and apply new materials into the spherical PhC systems to extend the functions of the PCBs, such as high specific and sensitivity to the external stimuli, large response level, and rapid response rate. Third, because of the interconnected macroporous structure, various potential applications of the PCBs for drug release, selective separations, fuel or solar cells, as well as catalyst supports are expected to be implemented. Fourth, although the bottom-up method of assembling monodisperse nanoparticles has great potential for the fabrication of PCBs, this approach has limited considerations because it is difficult to eliminate intrinsic defects in crystals and to achieve precise nanoparticle localization. Thus, the ideal PCBs for precise optical investigation including microlasers, low-loss resonators, and so on should be derived from the top-down approach. Finally, despite with many compelling concepts for their commercial value, the majority of the spherical PhCs-based technologies remain in the lab, facing a huge gap between research results and the requirements of real applications. To overcome this dilemma, it is important for the technology holders to cooperate with entrepreneurs to take the technology out of the lab. In a word, although there is still a long way to go, the shiny PC beads will have a shiny future.

AUTHOR INFORMATION

Corresponding Authors

*E-mail: yjzhao@seu.edu.cn (Y.J.Z.).
*E-mail: gu@seu.edu.cn (Z.Z.G.).

Notes

The authors declare no competing financial interest.

Biographies

Yuanjin Zhao received his Ph.D. degree in 2011 from Southeast University. Since 2012, he was promoted to be an associate professor of Southeast University. In 2009−2010, he worked as a research scholar at Prof. David A. Weitz's group at Harvard University. His research interests are focused on microfluidics and biomaterials.

Luoran Shang received his B.S. from Southeast University in 2013. She is now a Ph.D. candidate under the supervision of Prof. Yuanjin Zhao at Southeast University. Her research interest is in the fabrication of bioinspired photonic crystals.

Yao Cheng received his B.S. from Southeast University in 2010. She is now a Ph.D. candidate under the supervision of Prof. Zhongze Gu at Southeast University. Her research interest is in developing of functional materials by microfluidics.

Zhongze Gu received his Ph.D. degree in 1998 from the University of Tokyo under the direction of Professor Akira Fujishima. Then he started an academic career in KAST as a researcher. From 2003, he has been a Cheung Kong Scholars professor of Southeast University. Now he is the director of State Key Laboratory of Bioelectronics, China. His research interests include bioinspired photonic nanomaterials and biosensors.

ACKNOWLEDGMENTS

This work was supported by the National Science Foundation of China (Grant Nos. 21473029, 21105011, and 91227124), the National Science Foundation of Jiangsu (Grant No. BK20140028), and the Program for Changjiang Scholars and Innovative Research Team in University (IRT1222).

REFERENCES

(1) Freymann, G.; Kitaev, V.; Lotsch, B. V.; Ozin, G. A. Bottom-up assembly of photonic crystals. *Chem. Soc. Rev.* **2013**, *42*, 2528−2554.
(2) Zhang, Y. Z.; Wang, J. X.; Huang, Y.; Song, Y. L.; Jiang, L. Fabrication of functional colloidal photonic crystals based on well-designed latex particles. *J. Mater. Chem.* **2011**, *21*, 14113−14126.
(3) Wang, J. X.; Zhang, Y. Z.; Wang, S. T.; Song, Y. L.; Jiang, L. Bioinspired Colloidal Photonic Crystals with Controllable Wettability. *Acc. Chem. Res.* **2011**, *44*, 405−415.
(4) He, L.; Wang, M. S.; Ge, J. P.; Yin, Y. D. Magnetic Assembly Route to Colloidal Responsive Photonic Nanostructures. *Acc. Chem. Res.* **2012**, *45*, 1431−1440.
(5) Sato, O.; Kubo, S.; Gu, Z. Z. Structural Color Films with Lotus Effects, Superhydrophilicity, and Tunable Stop-Bands. *Acc. Chem. Res.* **2009**, *42*, 1−10.
(6) Zhao, Y. J.; Xie, Z. Y.; Gu, H. C.; Zhu, C.; Gu, Z. Z. Bio-inspired variable structural color materials. *Chem. Soc. Rev.* **2012**, *41*, 3297−3317.
(7) Velev, O. D.; Lenhoff, A. M.; Kaler, E. W. A Class of Microstructured Particles Through Colloidal Crystallization. *Science* **2000**, *287*, 2240−2243.
(8) Velev, O. D.; Gupta, S. Materials fabricated by micro- and nanoparticle assembly—The challenging path from science to engineering. *Adv. Mater.* **2009**, *21*, 1897−1905.
(9) Zhao, X. W.; Cao, Y.; Ito, F.; Chen, H. H.; Nagai, K.; Zhao, Y. H.; Gu, Z. Z. Colloidal crystal beads as supports for biomolecular screening. *Angew. Chem., Int. Ed.* **2006**, *45*, 6835−6838.
(10) Rastogi, V.; Melle, S.; Calderon, O. G.; Garcia, A. A.; Marquez, M.; Velev, O. D. Synthesis of light-diffracting assemblies from microspheres and nanoparticles in droplets on a superhydrophobic surface. *Adv. Mater.* **2008**, *20*, 4263−4268.
(11) Sun, C.; Zhao, X. W.; Zhao, Y. J.; Zhu, R.; Gu, Z. Z. Fabrication of colloidal crystal beads by a drop-breaking technique and their application as bioassays. *Small* **2008**, *4*, 592−596.
(12) Gu, H. C.; Rong, F.; Tang, B. C.; Zhao, Y. J.; Fu, D. G.; Gu, Z. Z. Photonic Crystal Beads from Gravity-Driven Microfluidics. *Langmuir* **2013**, *29*, 7576−7582.
(13) Kim, S. H.; Lee, S. Y.; Yi, G. R.; Pine, D. J.; Yang, S. M. Microwave-Assisted Self-Organization of Colloidal Particles in Confining Aqueous Droplets. *J. Am. Chem. Soc.* **2006**, *128*, 10897−10904.
(14) Xu, K.; Xu, J. H.; Lu, Y. C.; Luo, G. S. Extraction-Derived Self-Organization of Colloidal Photonic Crystal Particles within Confining Aqueous Droplets. *Cryst. Growth Des.* **2013**, *13*, 926−935.
(15) Zhao, Y. J.; Zhao, X. W.; Sun, C.; Li, J.; Zhu, R.; Gu, Z. Z. Encoded silica colloidal crystal beads as supports for potential multiplex immunoassay. *Anal. Chem.* **2008**, *80*, 1598−1605.
(16) Hu, J.; Zhao, X. W.; Zhao, Y. J.; Li, J.; Xu, W. Y.; Wen, Z. Y.; Xu, M.; Gu, Z. Z. Photonic crystal hydrogel beads used for multiplex biomolecular detection. *J. Mater. Chem.* **2009**, *19*, 5730−5736.
(17) Ge, J. P.; Lee, H.; He, L.; Kim, J.; Lu, Z. D.; Kim, H.; Goebl, J.; Kwon, S.; Yin, Y. D. Magnetochromatic Microspheres: Rotating Photonic Crystals. *J. Am. Chem. Soc.* **2009**, *131*, 15687−15694.
(18) Kanai, T.; Lee, D.; Shum, H. C.; Weitz, D. A. Fabrication of Tunable Spherical Colloidal Crystals Immobilized in Soft Hydrogels. *Small* **2010**, *6*, 807−810.

(19) Kim, S. H.; Jeon, S. J.; Yi, G. R.; Heo, C. J.; Choi, J. H.; Yang, S. M. Optofluidic Assembly of Colloidal Photonic Crystals with Controlled Sizes, Shapes, and Structures. *Adv. Mater.* **2008**, *20*, 1649−1655.
(20) Zhao, Y. J.; Zhao, X. W.; Tang, B. C.; Xu, W. Y.; Li, J.; Hu, J.; Gu, Z. Z. Quantum-Dot-Tagged Bioresponsive Hydrogel Suspension Array for Multiplex Label-Free DNA Detection. *Adv. Funct. Mater.* **2010**, *20*, 976−982.
(21) Kim, Y. C.; Cho, C. Y.; Kang, J. H.; Cho, Y. S.; Moon, J. H. Synthesis of Porous Carbon Balls from Spherical Colloidal Crystal Templates. *Langmuir* **2012**, *28*, 10543−10550.
(22) Wang, J. Y.; Hu, Y. D.; Deng, R.; Liang, R. J.; Li, W. K.; Liu, S. Q.; Zhu, J. T. Multiresponsive Hydrogel Photonic Crystal Microparticles with Inverse-Opal Structure. *Langmuir* **2013**, *29*, 8825−8834.
(23) Cui, J. C.; Zhu, W.; Gao, N.; Li, J.; Yang, H. W.; Jiang, Y.; Seidel, P.; Ravoo, B. J.; Li, G. T. Inverse Opal Spheres Based on Polyionic Liquids as Functional Microspheres with Tunable Optical Properties and Molecular Recognition Capabilities. *Angew. Chem., Int. Ed.* **2014**, *53*, 3844−3848.
(24) Yi, G. R.; Moon, J. H.; Yang, S. M. Ordered Macroporous Particles by Colloidal Templating. *Chem. Mater.* **2001**, *13*, 2613−2618.
(25) Moon, J. H.; Yi, G. R.; Yang, S. M.; Pine, D. J.; Park, S. B. Electrospray-Assisted Fabrication of Uniform Photonic Balls. *Adv. Mater.* **2004**, *16*, 605−609.
(26) Zhao, Y. J.; Zhao, X. W.; Hu, J.; Xu, M.; Zhao, W. J.; Sun, L. J.; Zhu, C.; Xu, H.; Gu, Z. Z. Encoded Porous Beads for Label-Free Multiplex Detection of Tumor Markers. *Adv. Mater.* **2009**, *21*, 569−572.
(27) Yang, Q.; Li, M. Z.; Liu, J.; Shen, W. Z.; Ye, C. Q.; Shi, X. D.; Jiang, L.; Song, Y. L. Hierarchical TiO_2 photonic crystal spheres prepared by spray drying for highly efficient photocatalysis. *J. Mater. Chem. A* **2013**, *1*, 541−547.
(28) Millman, J. R.; Bhatt, K. H.; Prevo, B. G.; Velev, O. D. Anisotropic particle synthesis in dielectrophoretically controlled microdroplet reactors. *Nat. Mater.* **2005**, *4*, 98−102.
(29) Rastogi, V.; Garcıa, A. A.; Marquez, M.; Velev, O. D. Anisotropic Particle Synthesis Inside Droplet Templates on Superhydrophobic Surfaces. *Macromol. Rapid Commun.* **2010**, *31*, 190−195.
(30) Shang, L. R.; Shangguan, F. Q.; Cheng, Y.; Lu, J.; Xie, Z. Y.; Zhao, Y. J.; Gu, Z. Z. Microfluidic Generation of Magnetoresponsive Janus Photonic Crystal Particles. *Nanoscale* **2013**, *5*, 9553−9557.
(31) Yu, Z. Y.; Wang, C. F.; Ling, L. T.; Chen, L.; Chen, S. Triphase Microfluidic-Directed Self-Assembly: Anisotropic Colloidal Photonic Crystal Supraparticles and Multicolor Patterns Made Easy. *Angew. Chem., Int. Ed.* **2012**, *51*, 2375−2378.
(32) Zhao, Y. J.; Gu, H. C.; Xie, Z. Y.; Shum, H. C.; Wang, B. P.; Gu, Z. Z. Bio-inspired Multifunctional Janus Particles for Droplets Manipulation. *J. Am. Chem. Soc.* **2013**, *135*, 54−57.
(33) Kim, S. H.; Jeon, S. J.; Yang, S. M. Optofluidic Encapsulation of Crystalline Colloidal Arrays with Spherical Membranes. *J. Am. Chem. Soc.* **2008**, *130*, 6040−6046.
(34) Kim, S. H.; Park, J. G.; Choi, T. M.; Manoharan, V. N.; Weitz, D. A. Osmotic-pressure-controlled concentration of colloidal particles in thin-shelled capsules. *Nat. Commun.* **2014**, *5*, 3068.
(35) Hu, Y. D.; Wang, J. Y.; Wang, H.; Wang, Q.; Zhu, J. T.; Yang, Y. J. Microfluidic Fabrication and Thermoreversible Response of Core/Shell Photonic Crystalline Microspheres Based on Deformable Nanogels. *Langmuir* **2012**, *28*, 17186−17192.
(36) Kanai, T.; Lee, D.; Shum, H. C.; Shah, R. K.; Weitz, D. A. Gel-Immobilized Colloidal Crystal Shell with Enhanced Thermal Sensitivity at Photonic Wavelengths. *Adv. Mater.* **2010**, *22*, 4998−5002.
(37) Ye, B. F.; Ding, H. B.; Cheng, Y.; Gu, H. C.; Zhao, Y. J.; Xie, Z. Y.; Gu, Z. Z. Photonic crystal microcapsules for label-free multiplex detection. *Adv. Mater.* **2014**, *26*, 3270−3274.
(38) Gu, H. C.; Zhao, Y. J.; Cheng, Y.; Xie, Z. Y.; Rong, F.; Li, J. Q.; Wang, B. P.; Fu, D. G.; Gu, Z. Z. Tailoring Colloidal Photonic Crystals with Wide Viewing Angle. *Small* **2013**, *9*, 2266−2271.
(39) Kuang, M. X.; Wang, J. X.; Bao, B.; Li, F. Y.; Wang, L. B.; Jiang, L.; Song, Y. L. Inkjet Printing Patterned Photonic Crystal Domes for Wide Viewing-angle Displays by Controlling the Sliding Three Phase Contact Line. *Adv. Opt. Mater.* **2014**, *2*, 34−38.
(40) Kim, S. H.; Jeon, S. J.; Jeong, W. C.; Park, H. S.; Yang, S. M. Optofluidic Synthesis of Electro-responsive Photonic Janus Balls with Isotropic Structural Colors. *Adv. Mater.* **2008**, *20*, 4129−4134.
(41) Zhu, C.; Xu, W. Y.; Chen, L. S.; Zhang, W. D.; Xu, H.; Gu, Z. Z. Magnetochromatic Microcapsule Arrays for Displays. *Adv. Funct. Mater.* **2011**, *21*, 2043−2048.
(42) Zhao, Y. J.; Zhao, X. W.; Gu, Z. Z. Photonic Crystals in Bioassays. *Adv. Funct. Mater.* **2010**, *20*, 2970−2988.
(43) Zhao, Y. J.; Zhao, X. W.; Pei, X. P.; Hu, J.; Zhao, W. J.; Chen, B. A.; Gu, Z. Z. Multiplex detection of tumor markers with photonic suspension array. *Anal. Chim. Acta* **2009**, *633*, 103−108.
(44) Zhao, Y. J.; Zhao, X. W.; Tang, B. C.; Xu, W. Y.; Gu, Z. Z. Rapid and Sensitive Biomolecular Screening with Encoded Macroporous Hydrogel Photonic Beads. *Langmuir* **2010**, *26*, 6111−6114.
(45) Zhao, Y. J.; Xie, Z. Y.; Gu, H. C.; Jin, L.; Zhao, X. W.; Wang, B. P.; Gu, Z. Z. Multifunctional photonic crystal barcodes from microfluidics. *NPG Asia Mater.* **2012**, *4*, e25.
(46) Xie, Z. Y.; Cao, K. D.; Zhao, Y. J.; Bai, L.; Gu, H. C.; Xu, H.; Gu, Z. Z. An Optical Nose Chip Based on Mesoporous Colloidal Photonic Crystal Beads. *Adv. Mater.* **2014**, *26*, 2413−2418.
(47) Zhao, Y. J.; Zhao, X. W.; Hu, J.; Li, J.; Xu, W. Y.; Gu, Z. Z. Multiplex Label-Free Detection of Biomolecules with an Imprinted Suspension Array. *Angew. Chem., Int. Ed.* **2009**, *48*, 7350−7352.
(48) Ge, J. P.; Yin, Y. D. Responsive Photonic Crystals. *Angew. Chem., Int. Ed.* **2011**, *50*, 1492−1522.
(49) Shen, W. Z.; Li, M. Z.; Ye, C. Q.; Jiang, L.; Song, Y. L. Directwriting colloidal photonic crystal microfluidic chips by inkjet printing for label-free protein detection. *Lab Chip* **2012**, *12*, 3089−3095.
(50) Ye, B. F.; Rong, F.; Gu, H. C.; Xie, Z. Y.; Cheng, Y.; Zhao, Y. J.; Gu, Z. Z. Bioinspired angle-independent photonic crystal colorimetric sensing. *Chem. Commun.* **2013**, *49*, 5331−5333.
(51) Liu, W.; Shang, L. R.; Zheng, F. Y.; Qian, J. L.; Lu, J.; Zhao, Y. J.; Gu, Z. Z. Photonic Crystal Encoded Microcarriers for Biomaterials Evaluation. *Small* **2014**, *10*, 88−93.
(52) Zheng, F. Y.; Cheng, Y.; Wang, J.; Lu, J.; Zhang, B.; Zhao, Y. J.; Gu, Z. Z. Aptamer-functionalized Barcode Particles for Capture and Detection of Multiple Types of Circulating Tumor Cells. *Adv. Mater.* **2014**, DOI: 10.1002/adma.201403530.